Speed from light: growth rate and bulk flow at z ∼ 0.1 from improved SDSS DR13 photometry

M. Feix, E. Branchini, A. Nusser

HAL Id: hal-01542815

https://hal.sorbonne-universite.fr/hal-01542815

Submitted on 20 Jun 2017

Speed from light: growth rate and bulk flow at $z \sim 0.1$ from improved SDSS DR13 photometry

M. Feix,[1]⋆ E. Branchini[2,3,4] and A. Nusser[5,6]

[1]*CNRS, UMR 7095 and UPMC, Institut d'Astrophysique de Paris, 98 bis Boulevard Arago, F-75014 Paris, France*
[2]*Department of Mathematics and Physics, Università Roma Tre, Via della Vasca Navale 84, Rome I-00146, Italy*
[3]*INFN Sezione di Roma 3, Via della Vasca Navale 84, Rome I-00146, Italy*
[4]*INAF, Osservatorio Astronomico di Roma, Monte Porzio Catone, I-00040, Italy*
[5]*Department of Physics, Israel Institute of Technology – Technion, Haifa 32000, Israel*
[6]*Asher Space Science Institute, Israel Institute of Technology – Technion, Haifa 32000, Israel*

ABSTRACT

Observed galaxy luminosities (derived from redshifts) hold information on the large-scale peculiar velocity field in the form of spatially correlated scatter, which allows for bounds on bulk flows and the growth rate of matter density perturbations using large galaxy redshift surveys. We apply this luminosity approach to galaxies from the recent SDSS Data Release 13. Our goal is twofold. First, we take advantage of the recalibrated photometry to identify possible systematic errors relevant to our previous analysis of earlier data. Second, we seek improved constraints on the bulk flow and the normalized growth rate $f\sigma_8$ at $z \sim 0.1$. Our results confirm the robustness of our method. Bulk flow amplitudes, estimated in two redshift bins with $0.02 < z_1 < 0.07 < z_2 < 0.22$, are generally smaller than in previous measurements, consistent with both the updated photometry and expectations for the Λ cold dark matter model. The obtained growth rate, $f\sigma_8 = 0.48 \pm 0.16$, is larger than, but still compatible with, its previous estimate, and closer to the reference value of Planck. Rather than precision, the importance of these results is due to the fact that they follow from an independent method that relies on accurate photometry, which is a top requirement for next-generation photometric catalogues.

Key words: methods: data analysis – methods: statistical – surveys – cosmological parameters – dark energy – dark matter – large-scale structure of Universe.

1 INTRODUCTION

Cosmology is steadily maturing from a phase driven by high precision to a high-accuracy science. While statistical estimators and observational strategies have been designed to minimize random errors, the focus is now shifting towards systematic uncertainties and their impact on the total error budget. Various strategies have been adopted to tackle this problem. The most effective one is to estimate the same quantity using different techniques applied to independent data sets. Considering the linear growth rate of matter density fluctuations, *f*, as an example, redshift-space distortions (RSDs) have been recognized as the most promising method to estimate this important quantity (e.g. Guzzo et al. 2008; Percival & White 2009) and are now adopted as its standard probe in next-generation galaxy redshift surveys (e.g. Laureijs et al. 2011; Levi et al. 2013). Peculiar velocities measured from distance indicators have traditionally represented an alternative probe that has provided a precious, though very local, robustness test for analyses based on RSDs. More recently, yet another technique has been proposed to infer the growth rate from a photometric data set complemented with spectroscopic redshift information (Nusser, Branchini & Davis 2012; Feix, Nusser & Branchini 2015). Thanks to this luminosity method, we now have independent and consistent *f*-estimates out to redshifts $z \sim 0.1$.

The luminosity method can also be used to assess the coherence of the peculiar velocity field, most notably the bulk flow, i.e. the volume average of the peculiar velocity field. Again, and this constitutes a second example, this technique has provided an important consistency check to other estimates based on galaxy peculiar velocities and contributed to rule out claims of anomalously large flows that would prove difficult to justify within the standard cosmological Λ cold dark matter (ΛCDM) scenario (Nusser, Branchini & Davis 2011; Branchini, Davis & Nusser 2012; Feix, Nusser & Branchini 2014).

The purpose of this paper is to further the luminosity method by reducing the impact of systematics and to improve estimates of the bulk flow and the cosmic growth rate at $z \sim 0.1$ obtained in Feix et al. (2015). We are able to achieve this goal using the

⋆ E-mail: feix@iap.fr

new Sloan Digital Sky Survey Data Release 13 (SDSS DR13) catalogue (SDSS Collaboration 2000, 2016) in which photometry has been recalibrated to a nominal mmag level (Finkbeiner et al. 2016). Accurate photometry is of paramount importance to bulk flows inferred from the luminosity method adopted here since small, but spatially correlated errors can mimic spurious coherent flows and lead to biased measurements.

We aim at two main goals. First, thanks to a reduction of systematic errors, we will test the robustness of our previous results. This mainly applies to the bulk flow estimate since the measurement of the growth rate involves additional information (spatial clustering from spectroscopic redshift surveys) which reduces the impact of systematics. Secondly, due to the fact that statistical uncertainties of the recalibrated magnitudes are also smaller, we will be able to improve the accuracy in the bulk flow estimate.

The paper is structured as follows: after a short recap of the luminosity methodology and its underlying equations in Section 2, we introduce the SDSS data and mock galaxy samples used by our analysis in Section 3. Considering galaxies in two different redshift bins, we present new bulk flow measurements and discuss their interpretation using mock catalogues in Section 4.1. Adopting clustering-based reconstructions of the linear velocity field, we provide updated constraints on the growth rate of density perturbations and compare these to previous findings in Section 4.2. Throughout this work, we will closely follow the notation of Feix et al. (2014, 2015), and assume a flat ΛCDM cosmology with fixed density parameters based on the *Wilkinson Microwave Anisotropy Probe* taken from Calabrese et al. (2013). Galaxy redshifts are expressed relative to the rest frame of the cosmic microwave background using the dipole estimate of Fixsen et al. (1996).

2 METHODOLOGY

To lowest order in linear perturbation theory, observed galaxy redshifts z differ from their actual cosmological distances or redshifts z_c, which are defined for an unperturbed background, according to (e.g. Sachs & Wolfe 1967)

$$\frac{z - z_c}{1 + z} \approx \frac{V(t, \hat{r}r)}{c}. \tag{1}$$

Here, $\hat{r}$ is a unit vector along the line of sight to a given galaxy and V denotes the physical radial peculiar velocity field that yields the predominant contribution to this difference at sufficiently low redshifts. Consequently, observed magnitudes M, derived from galaxy redshifts, are generally different from the true value $M^{(t)}$,

$$M = m - \mathrm{DM}(z) - K(z) + Q(z)$$

$$= M^{(t)} + 5 \log_{10} \frac{D_L(z_c)}{D_L(z)}, \tag{2}$$

where $\mathrm{DM} = 25 + 5 \log_{10}[D_L/\mathrm{Mpc}]$ is the distance modulus, D_L denotes the luminosity distance, m is the apparent magnitude and the functions $K(z)$ and $Q(z)$ account for K-corrections (e.g. Blanton & Roweis 2007) and luminosity evolution with redshift, respectively. The modulation of magnitudes $M - M^{(t)}$ is systematic across the sky and can be harnessed to obtain constraints on the peculiar velocity field, using maximum-likelihood techniques (Tammann, Yahil & Sandage 1979).

Detailed descriptions of the luminosity method and its various implementations are given in Nusser et al. (2011, 2012) and Feix et al. (2014). Here, we present a brief overview of the key elements. Considering a galaxy survey with magnitudes, spectroscopic redshifts and angular positions $\hat{r}_i$ on the sky, the starting point is to

choose an appropriate model for the radial velocity field $V(\hat{r}, z)$ that is characterized by a set of model parameters ζ_k. To find an estimate of the ζ_k, one maximizes the probability of observing the data,

$$P_{\mathrm{tot}} = \prod_i P\left(M_i | z_i, V_i(\{\zeta_k\})\right)$$

$$= \prod_i \left(\phi(M_i) \Big/ \int_{M_i^+}^{M_i^-} \phi(M)\mathrm{d}M\right), \tag{3}$$

where $V_i(\{\zeta_k\})$ corresponds to the radial velocity field evaluated at the position of galaxy i, and redshift errors are neglected (Nusser et al. 2011, 2012). Here, $\phi(M)$ denotes the galaxy luminosity function (LF) that is determined from the very same data set and $M^{\pm}$ are the limiting magnitudes that depend on the survey's flux cuts and individual radial velocities field through the cosmological redshift z_c specified in equation (1). The rationale of this approach is to find the set of model parameters that yield the minimal spread in the observed magnitudes.

The luminosity method may be used to constrain the peculiar velocity field in different ways. In this study, we focus on two types of measurements. To estimate cosmic bulk flows, we simply set the peculiar velocity model to $V(\hat{r}, z) = \hat{r} \cdot \boldsymbol{v}_B$, where the components of the bulk flow vector $\boldsymbol{v}_B$ are the free model parameters determined by the likelihood procedure (Nusser et al. 2011; Branchini et al. 2012). Since the peculiar velocity field is spatially coherent on large scales, another possibility is to independently predict it from the observed galaxy distribution in redshift space (Peebles 1980; Nusser & Davis 1994; Keselman & Nusser 2017). The velocity field obtained in this way is a function of $\beta = f/b$, where f is the growth rate and b is the linear bias between galaxies and total matter. Combined with the likelihood approach, this allows for constraining β with observed galaxy luminosities (Nusser et al. 2012).

An important element in the luminosity approach is to reliably estimate the galaxy LF from the given data. To this end, we adopt two different models of the LF in our analysis. The first one was introduced in Branchini et al. (2012) and is based on a cubic spline. Details regarding the implementation of this particular spline model are extensively discussed in Feix et al. (2014). The second one assumes the well-known Schechter form that is characterized by the usual parameters $M^{\star}$ and $\alpha^{\star}$ (Sandage, Tammann & Yahil 1979; Schechter 1980). As the normalization of the LF cancels in the likelihood function, it does not concern us here.

3 DATA

3.1 SDSS DR13 galaxy catalogue

The key asset of this work is the recently improved SDSS galaxy photometry of the publicly available DR13 (SDSS Collaboration 2016).[1] Considering only galaxies that are part of the SDSS legacy survey, the catalogue has a median redshift of $z \approx 0.1$ and provides magnitudes in five different photometric bands which are corrected for Galactic extinction using the updated estimates of Schlafly & Finkbeiner (2011). Compared to previous data releases, the SDSS photometry has been recalibrated using imaging data from the PanSTARRS1 survey (Kaiser et al. 2010) yielding differences up to the percent level (Finkbeiner et al. 2016). Analogue to our recent

---

[1] http://www.sdss.org/dr13/

analysis based on galaxies from the SDSS DR7 (SDSS Collaboration 2009; Feix et al. 2014), we use Petrosian *r*-band magnitudes and select galaxies within $14.5 < m_r < 17.6$. Furthermore, we exclude galaxies with questionable spectroscopic redshifts or photometry by requiring the corresponding zWarning and PS1_UNPHOT flags to equal zero. Since it plays a negligible role in our analysis that is insensitive to galaxy clustering, we make no attempt at accounting for fibre collisions. To minimize systematic effects resulting from uncertainties in *K*-corrections or luminosity evolution, we express absolute magnitudes in the $^{0.1}r$ bandpass (Blanton et al. 2003a). Finally, we further constrain the observed absolute magnitudes M_r and redshifts of galaxies by imposing $-22.5 < M_r - 5\log_{10}h < -17.0$ and $0.02 < z < 0.22$. For our assumed cosmology, this yields a working sample with approximately 4.5×10^5 galaxies, comprising around 10^5 galaxies less than the corresponding SDSS DR7 sample considered in Feix et al. (2014). This purer sample is labelled as luminosityA and used for the bulk flow measurements presented in Section 4.1.

Concerning the constraints on β, we also constructed a second flux-limited subsample, luminosityB, which was obtained as in Feix et al. (2015) by trimming the sample luminosityA to the redshift range $0.06 < z < 0.12$ and selecting only galaxies within $-33° < \eta < 36°$ and $-48° < \lambda < 51.5°$, where η and λ are the SDSS survey latitude and survey longitude, respectively. This leads to a spatially connected sample volume at $z = 0.1$ for which reliable reconstructions of the peculiar velocity field can be obtained. The sample contains a total of roughly 1.7×10^5 galaxies, which is around 15 per cent less compared to the size of the data sample used in Feix et al. (2015).

Because we are dealing with galaxy samples limited to $z \approx 0.2$, we follow the lines of Feix et al. (2014) and assume that the luminosity evolution depends linearly on redshift, i.e.

$$Q(z) = Q_0 \times (z - z_0), \qquad (4)$$

where the pivotal redshift is set to $z_0 = 0.1$. Results from applying the luminosity method to these data sets are robust with respect to different models for luminosity evolution as well as *K*-corrections of individual galaxies (Feix et al. 2014). Regarding the latter, we shall adopt the two-dimensional polynomial model of Chilingarian, Melchior & Zolotukhin (2010) which yields *K*-corrections as a function of redshift and $g - r$ colour. To compute limiting absolute magnitudes $M^\pm$ at a given redshift z in the $^{0.1}r$ bandpass, we resort to the mean *K*-correction specified in Feix et al. (2014). Like in our previous analyses based on DR7, galaxies are weighted by their angular completeness when calculating the total likelihood function P_{tot}.

3.2 Mock galaxy catalogues

To aid the interpretation of bulk flow measurements, we consider a suite of 269 mock galaxy catalogues that were modelled after the SDSS DR7 and allow for an assessment of effects due to known systematics, incompleteness and cosmic variance. A detailed description of how these mocks were constructed can be found in Feix et al. (2014). Since the number of galaxies in the DR7 and DR13 samples is comparable and the photometric recalibration of *r*-band magnitudes in DR13 introduced only slight changes at the level of a few mmag, the mock catalogues remain a suitable choice for the present study. Cross-matching DR13 and DR7 galaxies within 1 arcsec, for example, we find that more than 95 per cent of all galaxies in luminosityA are included in the corresponding DR7 sample of Feix et al. (2014). As we show in Section 4.1, a further
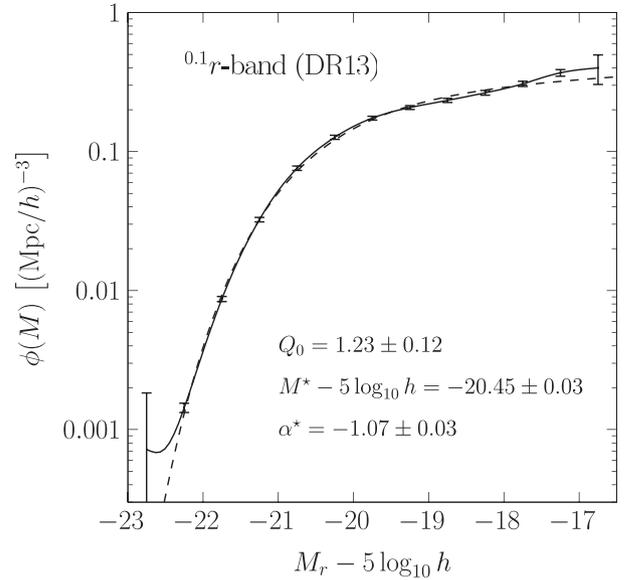

Figure 1. The $^{0.1}r$-band LF of the luminosityA sample from the SDSS DR13: illustrated are the maximum-likelihood result adopting the spline-based estimator with $\Delta M = 0.5$ (solid line), and a fit based on the Schechter model (dashed line). Error bars correspond to marginalized 99.7 per cent confidence limits of individual spline points.

indication is provided by a very similar LF estimate between the two data sets.

The mock catalogues include a systematic error in the SDSS DR7 photometric calibration which results in an overall zero-point photometric tilt at the level of 10 mmag over the entire survey area (Padmanabhan et al. 2008). This tilt was modelled by a randomly oriented dipole which is characterized by a root mean square of $\delta m_{\text{dipole}} = 0.01$ using all galaxies in the sample. Since the impact of such systematics is expected to be significantly reduced in the new SDSS DR13 calibration (Finkbeiner et al. 2016), we have removed the dipole contribution from all mocks before considering them in our analysis.

4 DATA ANALYSIS

In what follows, we apply the luminosity method to the SDSS DR13 galaxy samples. The new bulk flow measurements are presented and interpreted in Section 4.1 and updated constraints on the cosmic growth rate are discussed in 4.2. For both cases, we will compare our results to previous estimates based on the corresponding SDSS DR7 data sets (Feix et al. 2014, 2015).

4.1 Bulk flow estimates

To begin with, we determine the LF, denoted by $\phi(M)$, in the $^{0.1}r$ band for the sample luminosityA, assuming a vanishing velocity field. Choosing the spline-based estimator with a spline-point separation of $\Delta M = 0.5$, the result is illustrated as the solid line in Fig. 1. Just as in Feix et al. (2014), $\phi(M)$ is normalized to unity over the sample's absolute magnitude range, and the error bars were obtained from the 'constrained' covariance matrix that enforces the normalization constraint by a Lagrangian multiplier (James 2006). Despite a smaller estimate of the evolution parameter, $Q_0 = 1.23 \pm 0.12$ (1.60 ± 0.11 for DR7), the result obtained agrees well with studies based on previous data releases (Blanton

Table 1. Comparison of bulk flow measurements obtained from the SDSS DR7 and DR13 galaxy samples in two redshift bins for the different models of the LF described in the text. The quoted errors represent marginalized 68 per cent confidence intervals.

$\phi(M)$	$0.02 < z < 0.07$			$0.07 < z < 0.22$			
	v_x (km s^{-1})	v_y (km s^{-1})	v_z (km s^{-1})	v_x (km s^{-1})	v_y (km s^{-1})	v_z (km s^{-1})	
Hybrid	-227 ± 128	-326 ± 113	-239 ± 73	-367 ± 92	-439 ± 85	-25 ± 71	
Fixed	-175 ± 126	-278 ± 111	-147 ± 58	-340 ± 90	-409 ± 81	-45 ± 43	(DR7)
Schechter	-151 ± 130	-277 ± 116	-102 ± 78	-422 ± 93	-492 ± 86	-150 ± 74	
Hybrid	-200 ± 140	-292 ± 122	-146 ± 84	-349 ± 100	-301 ± 92	129 ± 87	
Fixed	-199 ± 140	-292 ± 121	-129 ± 61	-363 ± 100	-323 ± 90	70 ± 47	(DR13)
Schechter	-202 ± 141	-287 ± 124	69 ± 92	-356 ± 100	-324 ± 92	19 ± 93	

et al. 2003b; Montero-Dorta & Prada 2009; Feix et al. 2014). Fitting our estimate of $\phi(M)$ with a Schechter form, we obtain the parameters $M^\star - 5\log_{10}h = -20.45 \pm 0.03$ and $\alpha^\star = -1.07 \pm 0.03$, which is fully consistent with the analysis of SDSS DR7 data in Feix et al. (2014) and supports the argument in Section 3.2. The corresponding Schechter fit is shown as the dashed line in Fig. 1.

Since the SDSS samples cover only part of the sky, bulk flow measurements generally probe linear combinations of different velocity moments due to statistical mixing. This also includes the LF model and its evolution that may effectively introduce an additional monopole term. If interpreted with appropriate mock catalogues mimicking the angular footprint of the real survey, however, such measurements can yield meaningful results. Here, we shall follow the strategy described in Feix et al. (2014) to estimate bulk flows in two redshift bins with $0.02 < z_1 < 0.07 < z_2 < 0.22$.[2] In particular, we consider the following different approaches regarding the treatment of the LF in the likelihood analysis:

(i) Estimate the LF with the spline-based model for a vanishing velocity field, and keep it fixed in the subsequent bulk flow analysis.
(ii) Fit a Schechter form to the spline-based LF estimate for a vanishing velocity field and model the LF as a superposition of a Schechter form and the corresponding residual (hybrid approach).
(iii) Adopt a Schechter model for the LF.

The inferred bulk flows are summarized in Table 1. For comparison, we also list the recent estimates based on SDSS DR7 (Feix et al. 2014). The components of the bulk flow are expressed in a Cartesian coordinate system defined by its x-, y- and z-axes pointing towards Galactic coordinates $(l, b) \approx (81°, -7°)$, $(172°, -1°)$ and $(90°, 83°)$, respectively, where the z-axis roughly aligns with the direction towards the centre of the northern survey region. Measurement errors were derived from the covariance matrix $\mathbf{\Sigma}$ that is obtained by direct inversion of the observed Fisher matrix, defined as $\mathbf{F}_{\alpha\beta} = -\partial \log P_{\text{tot}}/(\partial x_\alpha \partial x_\beta)$ evaluated at the most likely parameter vector $\hat{x}^{\text{ML}}$.

Considering total bulk flow amplitudes, the DR13 estimates are generally smaller than the DR7 ones. Averaging the results over the different LF models yields values of $|\boldsymbol{v}_B| \approx 370 \pm 115$ and 485 ± 95 in units of km s^{-1} for the low- and high-redshift bin, respectively. In the high-z bin, the flow amplitudes are reduced by about 50–200 km s^{-1} compared to DR7, where the most significant changes appear for the Schechter model of the LF. The bulk flow components found from estimators using different LF models are in reasonable agreement, typically consistent within the quoted uncertainties. Assuming the results based on the hybrid model, the estimated bulk flows from DR13 are pointing towards $(l, b) \approx (315°,$
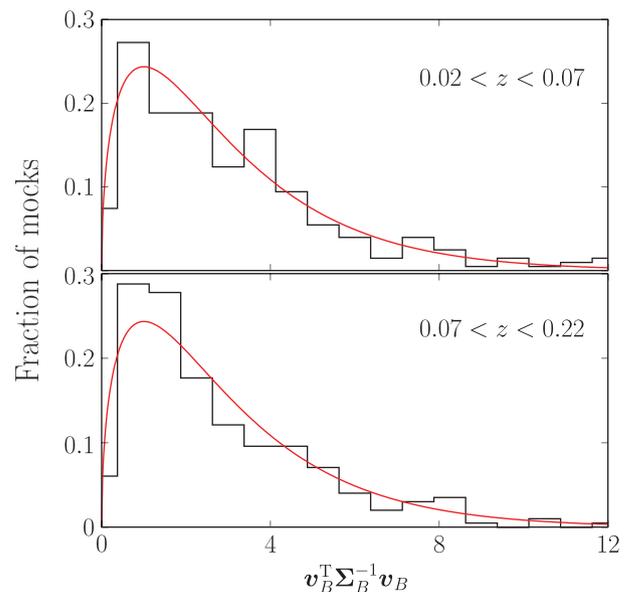
---

[2] As detailed in Feix et al. (2014), this choice mainly follows from requiring comparable signal-to-noise ratios between the two redshift bins.

Figure 2. Distribution of the quadratic form $\boldsymbol{v}_B^T \mathbf{\Sigma}_B^{-1} \boldsymbol{v}_B$ in two redshift bins derived from the SDSS mock catalogues, assuming the Schechter model of the LF: the histograms represent the observed (normalized) distribution and solid lines correspond to the χ^2-distribution with $k = 3$ degrees of freedom.

$-17°) \pm (52°, 15°)$ and $(304°, 22°) \pm (14°, 11°)$ for the first and second redshift bin, respectively. Similar directions are obtained for the other estimators.

To better assess these measurements, we repeated the analysis for the 269 mock galaxy catalogues introduced in Section 3.2. In contrast to the study presented in Feix et al. (2014), these mocks do not account for the photometric tilt of the SDSS DR7 calibration that severely contaminates bulk flows measured through the luminosity approach. The results based on our mocks suggest that the individual flow components obtained with our methods are not statistically independent, but subject to correlations at the level of 0.1–0.3. If the joint distribution of bulk flow components is approximately given by a multivariate Gaussian with covariance matrix $\mathbf{\Sigma}_B$, the quadratic form $\boldsymbol{v}_B^T \mathbf{\Sigma}_B^{-1} \boldsymbol{v}_B$ should follow a χ^2-distribution with $k = 3$ degrees of freedom. To test the validity of this assumption, we computed $\boldsymbol{v}_B^T \mathbf{\Sigma}_B^{-1} \boldsymbol{v}_B$ directly from the SDSS mocks. For the Schechter LF model, the resulting distributions, plotted as histograms in Fig. 2, are indeed well matched by the χ^2-distribution (solid curves). Adopting the other models of the LF yields very similar results. Using the estimate of $\mathbf{\Sigma}_B$ from the mock catalogues, we may therefore assign probabilities to the bulk flow measurements listed in Table 1. As customary, we express these in terms of confidence limits based on normally distributed data.

Table 2. Comparison of estimated event levels (expressed in standard deviations σ) for the bulk flow amplitudes obtained from the SDSS DR7 and DR13 galaxy samples in two redshift bins, assuming different LF models.

$\phi(M)$	Event level [σ]		
	$0.02 < z < 0.07$	$0.07 < z < 0.22$	
Hybrid	1.96	2.75	
Fixed	2.40	2.62	(DR7)
Schechter	0.95	3.19	
Hybrid	1.30	2.48	
Fixed	2.26	2.42	(DR13)
Schechter	1.18	2.22	

The corresponding event levels (in units of the standard deviation σ) for the inferred bulk flow amplitudes are presented in Table 2. Compared to the DR7 results, the probability estimates of the DR13 measurements are on average considerably larger, and thus consistent with an improved photometric calibration. The most prominent change is found in the high-z bin for the Schechter model of the LF, where the event level drops from 3.19 to 2.22σ. All measured DR13 flow amplitudes are contained within the 2.5σ confidence interval. Given the remaining uncertainties in the photometric data, limitations in the modelling of the mock catalogues, and their relatively small number, we conclude that the estimated bulk flows for SDSS DR13 are in agreement with the standard ΛCDM model. As was already pointed out in Feix et al. (2014), we emphasize that our results are robust with respect to the particular choices of the background cosmology,[3] K-corrections and the luminosity evolution.

4.2 Constraints on the growth rate at $z \sim 0.1$

Following the procedure outlined in Feix et al. (2015), we now derive constraints on β from the recalibrated SDSS DR13 data. The deviations in photometry between the bulk of DR13 and DR7 galaxies are around few mmag and have only little impact on the selection of volume-limited subsamples used to build models of the linear peculiar velocity field. Hence, we do not expect any relevant changes in the reconstruction of velocities that is generally robust to the adopted smoothing length and features on small scales (Nusser & Davis 1994; Nusser et al. 2012). For this reason, we resort to the velocity models of Feix et al. (2015) that were derived from the SDSS DR7 catalogue for discrete and equidistant β-values with $\Delta\beta = 0.05$ and $0 \leq \beta \leq 1$. These models are based on a decomposition of the smoothed galaxy density field into spherical harmonics ($l_{max} = 150$) and assume a Gaussian filter of $10\,h^{-1}$ Mpc radius. As argued in Feix et al. (2015), the contributions due to the monopole and dipole terms are uncertain and were removed from the velocity reconstruction ($l > 1$). Using the linear velocity models, galaxies in the subsample luminosityB are supplied with radial velocities $V_i(\beta)$ and then used in the likelihood procedure to determine the most probable β-value. To maximize P_{tot}, we adopt the spline-based LF that is fixed to its estimate for zero galaxy velocities. Our analysis also accounts for a slight statistical bias that emerges from the partial sky coverage of the considered SDSS data sets. All details regarding the calculation are summarized in Feix et al. (2014).

Carrying out the above steps, we find $\beta = 0.54 \pm 0.18$ for the DR13 galaxy sample. This new estimate is around 30 per cent
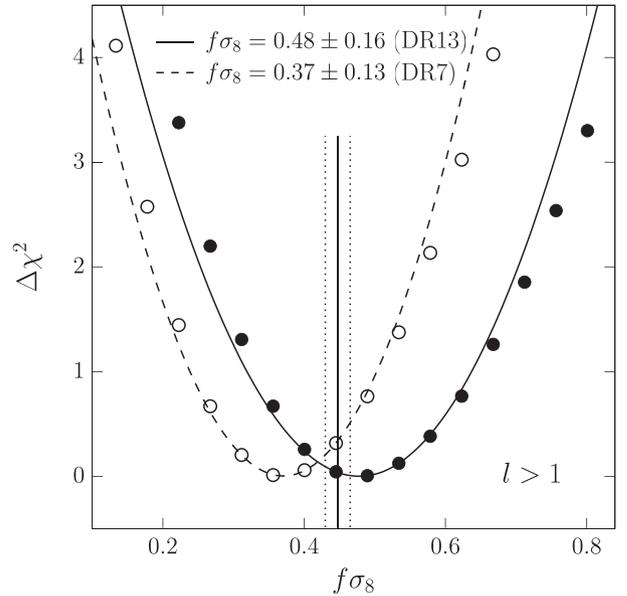
Figure 3. Estimated $\Delta\chi^2$ (and its quadratic approximation) as a function of $f\sigma_8$ for linear velocity models with $l > 1$. Presented are results based on galaxies from SDSS DR13 (filled circles) and DR7 (open circles). The estimates assume the power spectrum amplitude of $L^\star$-galaxies given by Tegmark et al. (2004). Vertical lines indicate the result inferred. from Planck data (TT + lowP + lensing; Planck Collaboration XIII 2016) and its 95 per cent confidence limits.

larger than our previous result ($\beta = 0.42 \pm 0.14$ for DR7), but consistent within the quoted uncertainties that have been obtained from approximating the log-likelihood near its maximum to quadratic order. For velocity models that exclude more of the low multipoles (e.g. models with $l > 5$), we observe a similar trend. Assuming the power spectrum amplitude of $L^\star$-galaxies inferred in Tegmark et al. (2004), we may rewrite the result in terms of $f\sigma_8$, which allows for a comparison to measurements based on different data sets (Song & Percival 2009) and where σ_8 is the amplitude of matter fluctuations in spheres of $8\,h^{-1}$ Mpc radius. This yields a value of $f\sigma_8 = 0.48 \pm 0.16$ (and $f\sigma_8 = 0.37 \pm 0.13$ for DR7; see Fig. 3) close to the ΛCDM estimate at $z = 0.1$ based on the Planck data ($f\sigma_8 \approx 0.45$; shown as the solid vertical line in Fig. 3; Planck Collaboration XIII 2016).

Our result is independent of the Hubble constant and quite insensitive to the precise choice of the cosmological parameters, the removal of high-l modes in the velocity models (Feix et al. 2015) or the used LF model. Assuming a Schechter form changes the result marginally, i.e. $\beta = 0.55 \pm 0.18$. Similar to the case of bulk flows, differences in the treatment of K-corrections and luminosity evolution have only a minor impact on the analysis (Nusser et al. 2012; Feix et al. 2014).

To summarize, the constraints on the large-scale peculiar velocity field at $z \sim 0.1$, derived from SDSS DR13 galaxies using the luminosity fluctuation method, are in excellent agreement with the standard ΛCDM model of cosmology. Compared to previous results obtained for DR7, measured bulk flow amplitudes are generally reduced, especially at higher redshifts ($0.07 < z < 0.22$) where photometric uncertainties have a more significant impact on the analysis. The estimated growth rate is slightly larger than, but still compatible with, the DR7 result, yielding a value close to the extrapolation based on Planck data. The found changes are consistent with the photometric recalibration of r-band magnitudes to a

nominal mmag level (Finkbeiner et al. 2016) and further confirm the robustness of the luminosity method for data sets with accurate photometry. From this point of view, all galaxy catalogues with similarly small photometric errors (Laureijs et al. 2011; LSST Dark Energy Science Collaboration 2012; Dark Energy Survey Collaboration 2016) could be considered for future applications.

REFERENCES

Blanton M. R., Roweis S., 2007, AJ, 133, 734
Blanton M. R. et al., 2003a, AJ, 125, 2348
Blanton M. R. et al., 2003b, ApJ, 592, 819
Branchini E., Davis M., Nusser A., 2012, MNRAS, 424, 472
Calabrese E. et al., 2013, Phys. Rev. D, 87, 103012
Chilingarian I. V., Melchior A.-L., Zolotukhin I. Y., 2010, MNRAS, 405, 1409
Dark Energy Survey Collaboration, 2016, MNRAS, 460, 1270
Feix M., Nusser A., Branchini E., 2014, J. Cosmol. Astropart. Phys., 9, 019
Feix M., Nusser A., Branchini E., 2015, Phys. Rev. Lett., 115, 011301
Finkbeiner D. P. et al., 2016, ApJ, 822, 66
Fixsen D. J., Cheng E. S., Gales J. M., Mather J. C., Shafer R. A., Wright E. L., 1996, ApJ, 473, 576
Guzzo L. et al., 2008, Nature, 451, 541
James F., 2006, Statistical Methods in Experimental Physics, 2nd edn. World Scientific Press, Singapore
Kaiser N. et al., 2010, in Stepp L. M., Gilmozzi R., Hall H. J., eds, Proc. SPIE Conf. Ser. Vol. 7733, Ground-based and Airborne Telescopes III. SPIE, Bellingham, p. 77330E
Keselman A., Nusser A., 2017, MNRAS, 467, 1915
Laureijs R. et al., 2011, preprint (arXiv:1110.3193)
Levi M. et al., 2013, preprint (arXiv:1308.0847)
LSST Dark Energy Science Collaboration, 2012, preprint (arXiv:1211.0310)
Montero-Dorta A. D., Prada F., 2009, MNRAS, 399, 1106
Nusser A., Davis M., 1994, ApJ, 421, L1
Nusser A., Branchini E., Davis M., 2011, ApJ, 735, 77
Nusser A., Branchini E., Davis M., 2012, ApJ, 744, 193
Padmanabhan N. et al., 2008, ApJ, 674, 1217
Peebles P. J. E., 1980, The Large-Scale Structure of the Universe. Princeton Univ. Press, Princeton, NJ
Percival W. J., White M., 2009, MNRAS, 393, 297
Planck Collaboration XIII, 2016, A&A, 594, A13
Sachs R. K., Wolfe A. M., 1967, ApJ, 147, 73
Sandage A., Tammann G. A., Yahil A., 1979, ApJ, 232, 352
Schechter P. L., 1980, AJ, 85, 801
Schlafly E. F., Finkbeiner D. P., 2011, ApJ, 737, 103
SDSS Collaboration, 2000, AJ, 120, 1579
SDSS Collaboration, 2009, ApJS, 182, 543
SDSS Collaboration, 2016, ApJS, preprint (arXiv:1608.02013)
Song Y.-S., Percival W. J., 2009, J. Cosmol. Astropart. Phys., 10, 4
Tammann G. A., Yahil A., Sandage A., 1979, ApJ, 234, 775
Tegmark M. et al., 2004, ApJ, 606, 702

This paper has been typeset from a TeX/LaTeX file prepared by the author.